

# Kinetic Modeling of Carbonylation of 1-(4-Isobutylphenyl)ethanol Using a Homogeneous $\text{PdCl}_2(\text{PPh}_3)_2/\text{TsOH}/\text{LiCl}$ Catalyst System

Abdul M. Seayad,<sup>†</sup> Jayasree Seayad,<sup>†</sup> Patrick L. Mills,<sup>‡</sup> and Raghunath V. Chaudhari<sup>\*,†</sup>

Homogeneous Catalysis Division, National Chemical Laboratory, Pune 411008, India, and Chemical Science and Engineering Laboratory, DuPont Company, Experimental Station, E304/A204, Wilmington, Delaware 19880-0304

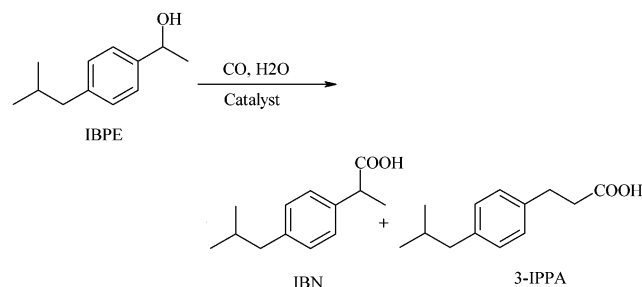
The kinetics of carbonylation of 1-(4-isobutylphenyl)ethanol (IBPE) were studied in a stirred semibatch reactor using a homogeneous  $\text{PdCl}_2(\text{PPh}_3)_2/\text{TsOH}/\text{LiCl}$  catalyst system. A three-step reaction pathway that describes the formation of an active palladium(0) species, the formation of active carbonylation substrate, 1-(4-isobutylphenyl)ethyl chloride, and the main carbonylation catalytic cycle has been proposed. The effect of the catalyst, (TsOH/LiCl) and IBPE concentrations and the partial pressure of CO on the rate and semibatch reactor performance has been investigated over the temperature range of 378–398 K. An empirical semibatch reactor model was derived, and the reaction rate parameters were evaluated based upon a simplified scheme. The rate model was found to satisfactorily predict the concentration versus time profiles at all temperatures. An attempt was also made to develop a dynamic model that accounts for the change in concentration of all of the catalytic intermediate species as well as the reactants and products.

## Introduction

Carbonylation reactions using homogeneous catalysis are gaining considerable interest for the synthesis of aldehydes, carboxylic acids, amino acids, and even novel polymeric materials, thereby providing new synthetic routes that may be not only more economical but also environmentally cleaner from a green chemistry perspective.<sup>1</sup> The carbonylation of alcohols and olefins to carboxylic acid derivatives is particularly suited for applications in fine chemicals and pharmaceutical industries because this catalytic route eliminates the use of stoichiometric reagents-based syntheses that otherwise generate large amounts of waste inorganic salts. In this context, carbonylation of aryl alcohols, especially 1-arylethanol, is of great significant importance because of its industrial application for the synthesis of 2-arylpropionic acids, which is a class of nonsteroidal antiinflammatory drugs. This route provides a cleaner alternative to a large variety of carboxylic acid products that are otherwise produced using cyanide reagents. Hoechst Celanese Corp. has first demonstrated this green chemistry route for the synthesis of ibuprofen (IBN) on a commercial scale by carbonylation of 1-(4-isobutylphenyl)ethanol (IBPE; Scheme 1) using a palladium complex catalyst,<sup>2</sup> which is often considered the best illustration of the role of catalysis in clean technologies. The minor side product formed is 3-(4-isobutylphenyl)propionic acid (3-IPPA).

In this process, either  $\text{PdCl}_2(\text{PPh}_3)_2$  or  $\text{PdCl}_2$  organometallic complexes in the presence of  $\text{PPh}_3$  were used as the catalyst system in a biphasic medium consisting of methyl ethyl ketone (MEK) as the organic phase and 10% aqueous HCl as the promoter at 5–35 MPa pressure and 403 K. The desired high selectivity (>98%) for the branched isomer, IBN, was achieved only at very

Scheme 1. Carbonylation of IBPE.



high pressures<sup>3</sup> (16–34 MPa) while lower selectivity (68%) was reported at low-pressure conditions (~6.8 MPa). In both cases, lower turnover frequencies (TOF = 40–175 h<sup>-1</sup>) were observed. Additives such as  $\text{CuCl}_2$  were reported to improve the selectivity under similar conditions.<sup>4</sup> A biphasic catalyst with a water-soluble palladium–TPPTS complex has also been recently reported; however, in this case very low reaction rates (TOF = 2.3 h<sup>-1</sup>) and lower IBN selectivity (70%) were also observed.<sup>5</sup> Our recent studies on the carbonylation of IBPE using Pd(II) complexes showed that the catalytic activity as well as the IBN selectivity were substantially enhanced when a combination of TsOH and LiCl were used as promoters under homogeneous conditions. For instance, an IBN selectivity of >95% and higher reaction rates (TOF = up to 1200 h<sup>-1</sup>) were achieved for the carbonylation of *p*-IBPE using  $\text{PdCl}_2(\text{PPh}_3)_2/\text{TsOH}/\text{LiCl}$  as the catalyst system with MEK solvent under 5.4 MPa CO pressure.<sup>6</sup>

While many reports have addressed the role of catalyst types, promoters, solvents and other reaction variables on the activity and selectivity behavior of this reaction, no published report has discussed the kinetics of this industrially important reaction. Knowledge of the intrinsic kinetics of the reaction and development of a suitable rate equation are important in understanding the reaction mechanism and for the optimal design of reactors for these processes. Also, this chemistry is a

\* To whom correspondence should be addressed. E-mail: rvc@ems.ncl.res.in. Tel: +91-20-5893163. Fax: +91-20-5893260.

<sup>†</sup> National Chemical Laboratory.

<sup>‡</sup> DuPont Co.

case of a gas–liquid catalytic reaction in which, in addition to the principal catalytic reaction, one or more of the promoters also catalyzes other reactions involving conversion of the catalyst precursor and substrate to active catalytic species. Interpretation of kinetic data and developing rate equations for such complex multi-step reaction systems presents a significant challenge. Therefore, the present work was undertaken with the goal of investigating the intrinsic kinetics of carbonylation of IBPE using a homogeneous catalyst system consisting of  $\text{PdCl}_2(\text{PPh}_3)_2/\text{PPh}_3$  as the catalyst precursor and  $\text{TsOH}/\text{LiCl}$  (1:1) as the promoter. The effect of various parameters such as catalyst loading, concentration of IBPE, excess water, promoters ( $\text{TsOH}/\text{LiCl}$ ), and the partial pressure of CO on the carbonylation rate as well as the concentration versus time profiles was studied in a temperature range of 378–398 K to develop rate equations and to evaluate the intrinsic kinetic parameters. The importance of dynamic reaction rate analysis that incorporates variation of the concentrations of the intermediate catalytic species for developing molecular level description of the kinetics has also been discussed.

## Experimental Section

The reactions for the kinetic study were carried out in a  $5 \times 10^{-5} \text{ m}^3$  (50 mL) Parr autoclave with wetted parts made of Hastelloy C-276 material. Ports were available for gas inlet and outlet, a rupture disk as a safety measure in case of excessive pressure buildup, and intermediate sampling. The temperature was controlled by an external heating jacket and a variable agitation speed was also utilized. The other experimental details of the reactor setup were the same as described in an earlier paper.<sup>7</sup> In a typical carbonylation reaction, known quantities of the substrate, catalyst, ligand, promoters, water, and solvent were charged to the autoclave. The reactor contents were flushed a few times with nitrogen followed by carbon monoxide and then heated to the desired temperature under low (10–20 rpm) stirring. After attaining the desired temperature, the autoclave was quickly pressurized with CO to a desired level and the reaction started by initiating a higher level of agitation (1000 rpm). To maintain a constant pressure in the reactor, CO was fed through a constant downstream pressure regulator from a reservoir vessel (100 mL). The pressure drop in the CO supply reservoir vessel was recorded by means of a pressure transducer as a function of time. Liquid samples were withdrawn from the reactor sampling port at regular intervals of time for offline analysis of the liquid reactants and products to obtain concentration versus time data. The analysis of the liquid samples was carried out using a gas chromatograph (GC; HP 5890) with a HP-FFAP capillary column [30 m  $\times$  0.32 mm  $\times$  0.1  $\mu\text{m}$  film thickness, on a poly(ethylene glycol) stationary phase]. The products were further characterized by GC–MS, NMR, and IR analysis.

## Results and Discussion

The main objective of this work was (i) to investigate the effect of different reaction and catalyst parameters on the rate of carbonylation of IBPE and to determine the potential effect of external mass transfer, (ii) to study the intrinsic kinetics of carbonylation of IBPE using the homogeneous palladium catalyst system  $\text{PdCl}_2(\text{PPh}_3)_2/\text{PPh}_3/\text{TsOH}/\text{LiCl}$ , and (iii) to develop rate

**Table 1. Range of Conditions Used for the Kinetic Study**

catalyst precursor, $\text{PdCl}_2(\text{PPh}_3)_2$ (kmol/ $\text{m}^3$ )	$1.121 \times 10^{-3}$ – $4.482 \times 10^{-3}$
$\text{PPh}_3$ (kmol/ $\text{m}^3$ )	$2.242 \times 10^{-3}$ – $8.964 \times 10^{-3}$
substrate, IBPE (kmol/ $\text{m}^3$ )	0.562–2.248
promoters, $\text{TsOH}/\text{LiCl}$ (1:1) (kmol/ $\text{m}^3$ )	0.224–0.896
partial pressure of CO (MPa)	3.4–7.48
temperature (K)	378–398
volume of the liquid phase ( $\text{m}^3$ )	$2.5 \times 10^{-5}$
agitation speed (rpm)	1000

equations representing the intrinsic kinetics of the reaction. For this purpose, several experiments were carried out in a semibatch mode in which concentration versus time data were obtained over a wide range of conditions as given in Table 1.

The carbonylation rates were evaluated from the rate of formation of total carboxylic acid and were stoichiometrically consistent with the rates obtained from CO consumption vs time plots as (eq 1):

$$r_A = \text{slope of} \\ \{\text{concentration of carbonylation products (IBN + 3-IPPA)}\} \text{ vs time plot} = \frac{d(C_{\text{IBN}} + C_{\text{3-IPPA}})}{dt} = \frac{V_G}{V_L RT} \frac{d(P_{\text{CO},0} - P_{\text{CO}})}{dt} \quad (1)$$

In all of the experiments, constant CO pressure and isothermal conditions were maintained. The material balance of IBPE and CO consumed was consistent (>96%) with the products [IBS, 1-(4-isobutylphenyl)-ethyl chloride (IBPECl), and IBN + IPPA] formed as per the stoichiometry given in Scheme 2. A typical concentration–time profile is shown in Figure 1. It was observed that, after the initial few minutes, the rate of formation of total carboxylic acid products was nearly constant for most of the reaction (15–60%).

**Solubility Data.** For interpretation of the kinetic data, knowledge of the CO solubility in MEK–IBPE liquid binary mixtures was required. The solubility of CO in mixtures of IBPE and MEK containing 4% of water was determined experimentally using a method described elsewhere.<sup>8</sup> The Henry's constants are given in Table 2. It was observed that the solubility of CO in the MEK–IBPE binary mixtures increased with temperature but decreased with an increase in the concentration of IBPE at all of the temperatures studied. The concentration of dissolved CO was calculated as  $A^* = P_{\text{CO}}H_e$ , where  $P_{\text{CO}}$  denotes the partial pressure of CO.

**Analysis of Mass-Transfer Effects.** Before using the experimental data for evaluation of the reaction kinetic parameters, two aspects were examined: (a) constancy of catalytic activity during an experiment and (b) significance of mass-transfer limitations. Catalyst recycle experiments were conducted by adding fresh IBPE to the final reaction mixture after complete conversion of the substrate. The results indicated negligible variation in the catalytic activity even after two recycles.

To assess the importance of mass-transfer limitations (gas–liquid mass transfer) for the gaseous reactant, the observed carbonylation rate data were compared with the maximum rates of gas–liquid mass transfer under the same conditions. The factor  $\alpha_1 = r_A/k_1aA^*$ , which quantifies the ratio of the rate observed to the maximum possible rate for gas–liquid mass transfer, was found to be less than 0.06 for the rate data in a temperature range of 378–398 K, which provides evidence that the

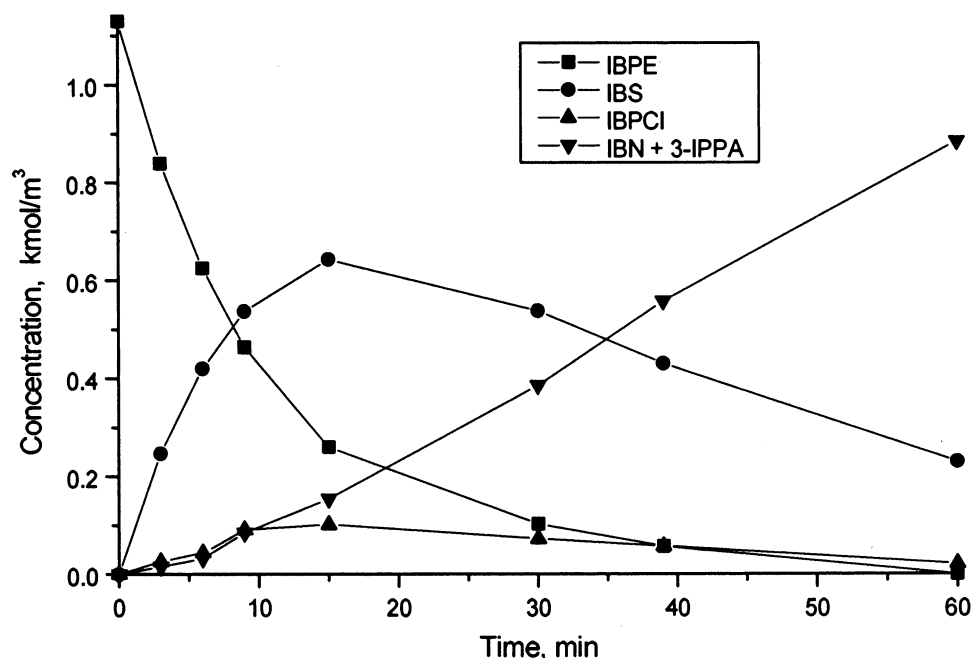


**Figure 1.** Typical concentration–time profile for carbonylation of IBPE. Reaction conditions: IBPE, 1.123 kmol/m<sup>3</sup>; TsOH/LiCl (1:1), 0.121 kmol/m<sup>3</sup>;  $P_{CO}$ , 5.4 MPa;  $PdCl_2(PPh_3)_2$ ,  $1.121 \times 10^{-3}$  kmol/m<sup>3</sup>; water, 2.67 kmol/m<sup>3</sup>; MEK,  $1.95 \times 10^{-5}$  m<sup>3</sup>.

**Scheme 2. Proposed Mechanistic Pathway for Carbonylation of IBPE**

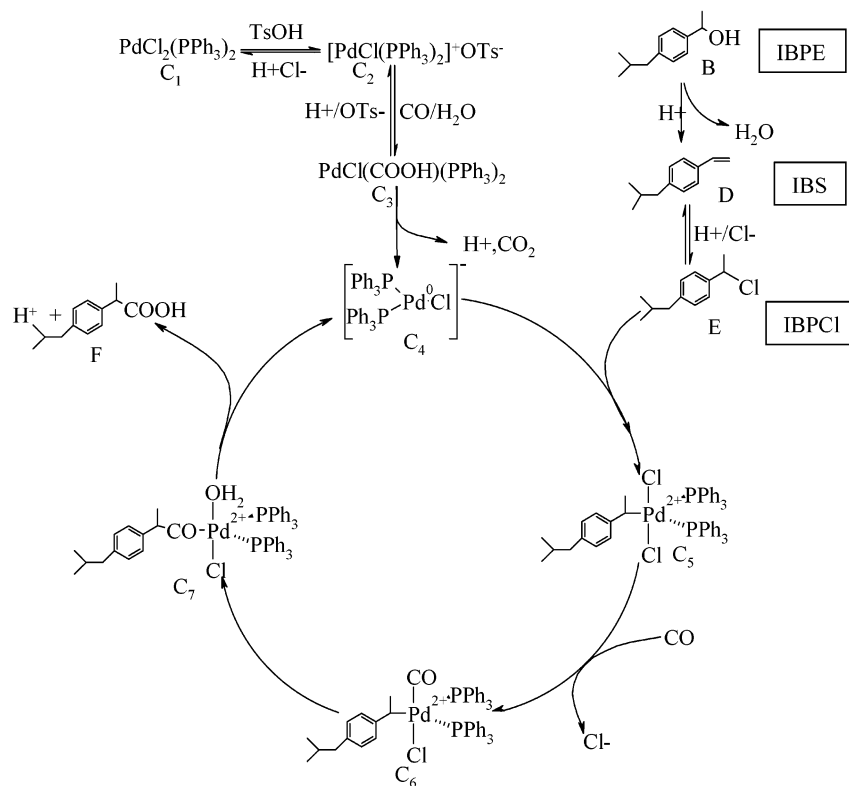


**Table 2. Henry's Constants of CO in a IBPE and MEK Mixture**

mixture of IBPE and MEK (w/w %)	$H_e \times 10^3$ (kmol/m <sup>3</sup> /MPa)		
	at 378 K	at 388 K	at 398 K
11% of IBPE	6.131	6.444	6.735
22% of IBPE	5.579	5.798	6.311
33% of IBPE	5.051	5.459	5.906

gas–liquid mass-transfer effects are negligible.<sup>9</sup> The effect of agitation speed on the rate of carbonylation was also studied at the highest catalyst loading at different temperatures (378, 388, and 398 K). These studies indi-

cated that, above 700 rpm, the agitation speed has no influence on the observed rate of carbonylation. These observations further support the conclusion that the gas–liquid mass-transfer resistance is not significant beyond 700 rpm. Hence, all of the experiments were carried out at an agitation speed of 1000 rpm to provide an additional margin for a negligible effect of external mass-transfer resistance.

**Initial Rate Data.** The kinetics of carbonylation of IBPE were studied in the temperature range of 378–398 K. The rate of carbonylation at the initial stage of

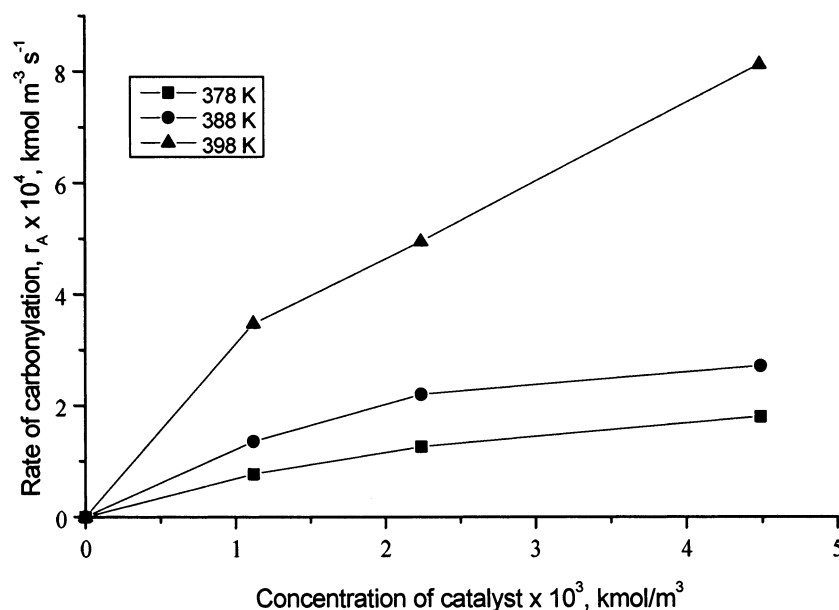


**Figure 2.** Effect of the concentration of catalyst on the rate of carbonylation of IBPE. Reaction conditions: IBPE, 1.123 kmol/m<sup>3</sup>; TsOH/LiCl (1:1), 0.121 kmol/m<sup>3</sup>;  $P_{CO}$ , 5.4 MPa; water, 2.67 kmol/m<sup>3</sup>; PPh<sub>3</sub>/Pd, 2; MEK,  $1.95 \times 10^{-5}$  m<sup>3</sup>.

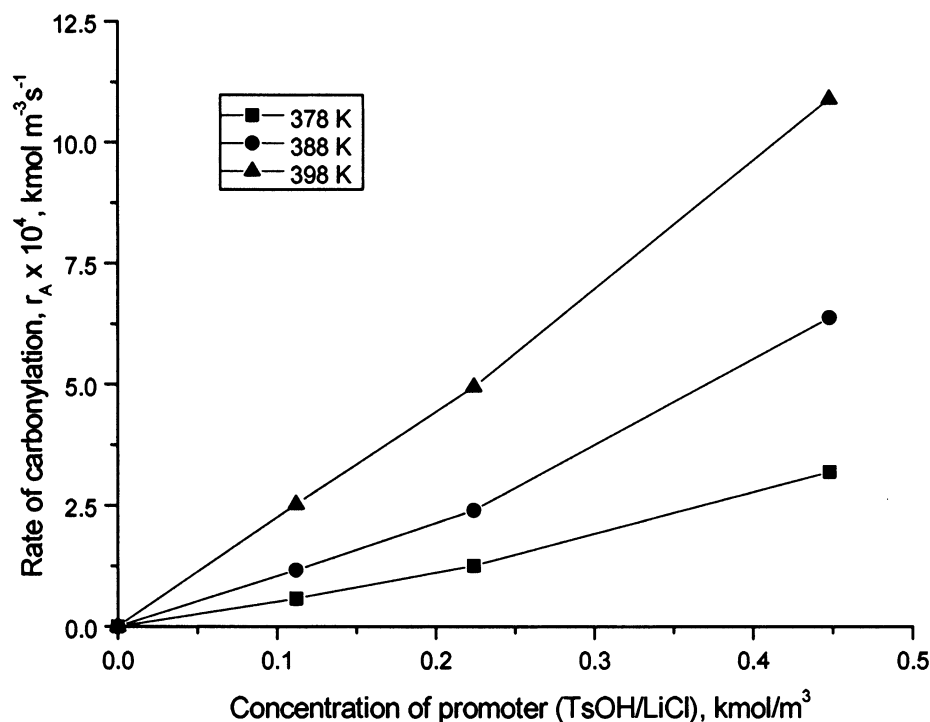


**Figure 3.** Effect of the concentration of promoter (TsOH/LiCl) on the rate of carbonylation of IBPE. Reaction conditions: IBPE, 1.123 kmol/m<sup>3</sup>; TsOH/LiCl, 1:1;  $P_{CO}$ , 5.4 MPa; PdCl<sub>2</sub>(PPh<sub>3</sub>)<sub>2</sub>,  $1.121 \times 10^{-3}$  kmol/m<sup>3</sup>; PPh<sub>3</sub>,  $2.242 \times 10^{-3}$  kmol/m<sup>3</sup>; water, 2.67 kmol/m<sup>3</sup>; MEK,  $1.95 \times 10^{-5}$  m<sup>3</sup>.

the reaction (within 5 min) was found to be very low, but this steadily increased and became almost constant after 5–10 min and then decreased slightly toward the end of the reaction. The lower initial reaction rate was attributed to a reduced rate of formation of the active carbonylation substrate IBPCl as well as that of the active catalytic species. Because the reaction involves more than one step, the initial rate data may not be very useful for the precise determination of the reaction kinetics. However, an average rate was calculated for every reaction at 5–25% conversion levels in order to understand the effect of different parameters on the general trends of carbonylation rates and to determine the apparent orders of reaction with respect to each species. For this purpose, the data after the initial

induction period were used. The rate of carbonylation was found to vary with 0.43th order with respect to the catalyst concentration as shown in Figure 2. This unusual trend of lower reaction order with respect to the catalyst concentration with the kinetic resistance controlling indicates that either the catalyst precursor may not be converted entirely to the active form or it may not be completely soluble in the reaction medium; the active catalyst may be in equilibrium with some less active or inactive palladium species; in such cases a fraction of the total catalyst charged will be available for catalysis, and thus a fractional order may result.

The average rate of carbonylation varied with an order of 1.2 with respect to the concentration of promoters (TsOH/LiCl at 1:1 ratio) and first order with respect

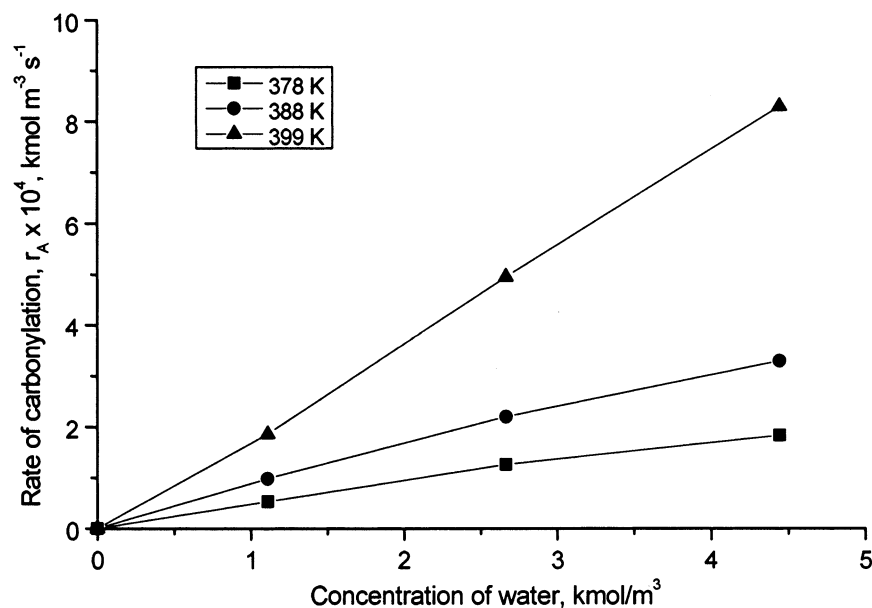


**Figure 4.** Effect of the concentration of water on the rate of carbonylation of IBPE. Reaction conditions: IBPE, 1.123 kmol/m<sup>3</sup>; TsOH/LiCl (1:1), 0.121 kmol/m<sup>3</sup>;  $P_{\text{CO}}$ , 5.4 MPa;  $\text{PdCl}_2(\text{PPh}_3)_2$ ,  $1.121 \times 10^{-3}$  kmol/m<sup>3</sup>;  $\text{PPh}_3$ ,  $2.242 \times 10^{-3}$  kmol/m<sup>3</sup>; MEK,  $1.95 \times 10^{-5}$  m<sup>3</sup>.

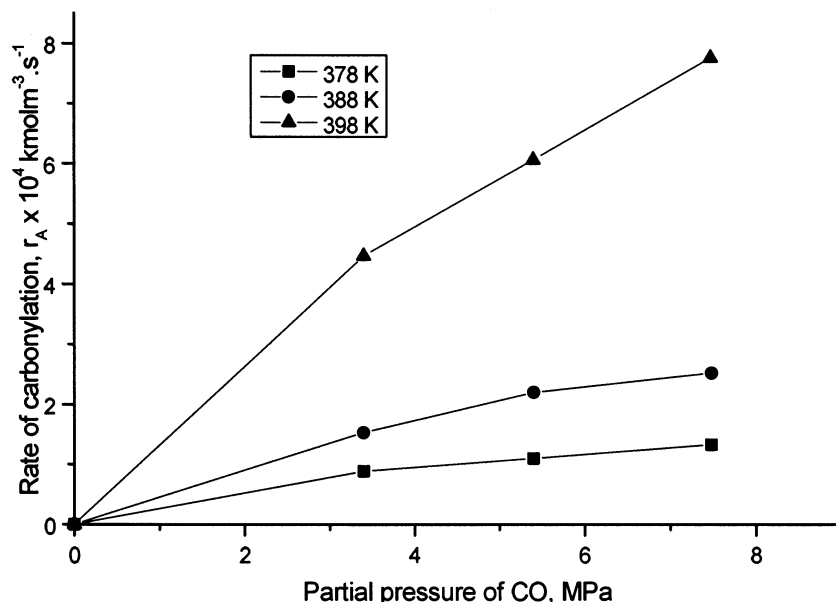


**Figure 5.** Effect of the partial pressure of CO on the rate of carbonylation of IBPE. Reaction conditions: IBPE, 1.123 kmol/m<sup>3</sup>; TsOH/LiCl (1:1), 0.121 kmol/m<sup>3</sup>;  $P_{\text{CO}}$ , 5.4 MPa;  $\text{PdCl}_2(\text{PPh}_3)_2$ ,  $1.121 \times 10^{-3}$  kmol/m<sup>3</sup>;  $\text{PPh}_3$ ,  $2.242 \times 10^{-3}$  kmol/m<sup>3</sup>; water, 2.67 kmol/m<sup>3</sup>; MEK,  $1.95 \times 10^{-5}$  m<sup>3</sup>.

to water as shown in Figures 3 and 4, respectively. The strong effect of the concentration of both promoter and water on the carbonylation rates indicates their active involvement in the formation of the active carbonylation substrate and/or the active catalytic species.

The average rate of carbonylation was also found to increase with an increase in the partial pressure of CO with an order of 0.8 (Figure 5) as well as the concentration of IBPE with an order of 0.7 (Figure 6).

**Mechanism of Reaction.** The overall carbonylation involves three independent steps<sup>10</sup> (Scheme 2), viz., (a) formation of the active substrate IBPCL (E), (b) activation of  $\text{PdCl}_2(\text{PPh}_3)_2$  to the active palladium(0) species ( $\text{C}_4$ ), and (c) catalytic carbonylation of IBPCL to IBN (F; the main catalytic cycle).

As described in Scheme 3, the active substrate that undergoes carbonylation is IBPCL, through IBS as the intermediate. It is well-known that the activation of

organic halides (R-X) by transition metals occurs by its oxidative addition to a low-valent metal complex.<sup>11</sup> In the case of palladium, it is a Pd(0) species to which the oxidative addition of R-X occurs to form a palladium(II) alkyl complex.<sup>12</sup> Hence, the Pd(II) catalyst precursor has to be reduced to an active Pd(0) species before the initiation of the catalytic cycle as described in our earlier paper.<sup>6</sup> The presence of weakly coordinating ions, such as  $\text{OTs}^-$ , may facilitate the formation of Pd(0) species from the precursor  $\text{PdCl}_2(\text{PPh}_3)_2$  through a type of water-gas shift reaction by the intervention of cationic species such as  $\text{C}_2$  as represented in Scheme 2. It is also well-known that in the presence of anions, such as halides ( $\text{Cl}^-$ ,  $\text{Br}^-$ ,  $\text{I}^-$ ), acetate ( $\text{OAc}^-$ ), etc., the low-ligated Pd(0) species formed will be present in the solution as anionic palladium species as  $[\text{Pd}^0(\text{PPh}_3)_2\text{Cl}]^-$ .<sup>13</sup> For the present case, the existence of anionic palladium complexes is most favored when compared to the low-



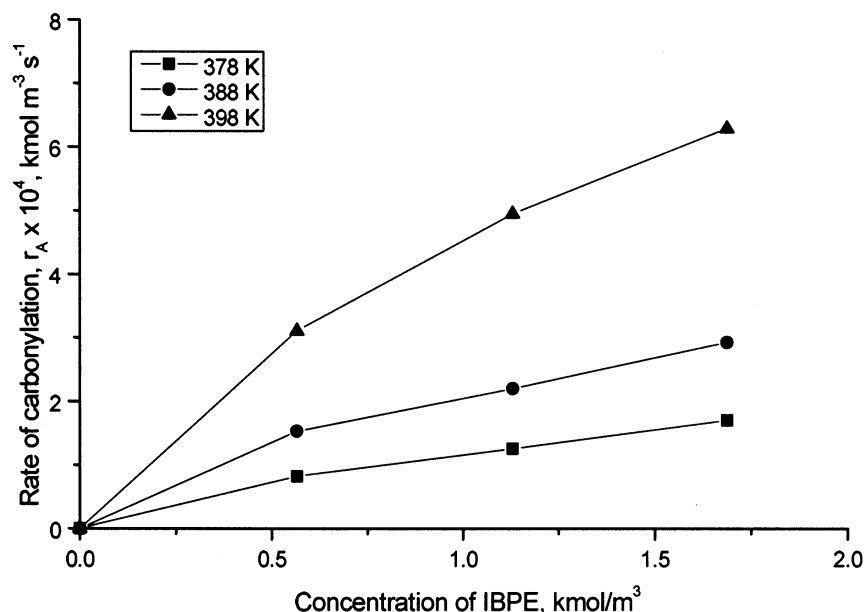


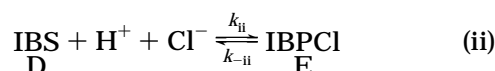
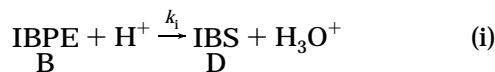
**Figure 6.** Effect of the concentration of IBPE on the rate of carbonylation of IBPE. Reaction conditions: TsOH/LiCl (1:1), 0.121 kmol/m³;  $P_{CO}$ , 5.4 MPa;  $PdCl_2(PPh_3)_2$ ,  $1.121 \times 10^{-3}$  kmol/m³;  $PPh_3$ ,  $2.242 \times 10^{-3}$  kmol/m³; water, 2.67 kmol/m³; MEK,  $1.95 \times 10^{-5}$  m³.

ligated Pd(0) species, and we propose a catalytic cycle (Scheme 2) based on  $[Pd^0(PPh_3)_2Cl]^-$  (species  $C_4$ ) as the active catalytic species. The anionic  $[Pd^0(PPh_3)_2Cl]^-$  may be stabilized by  $Li^+$  ions in the solution. The catalytic cycle starts by the oxidative addition of IBPE to the anionic species  $C_4$  to form a pentacoordinated palladium(II) alkyl complex,  $C_5$ . The greater nucleophilicity of the anionic Pd species compared to that of the Pd(0) species enhances the oxidative addition step.<sup>14</sup> The presence of  $Li^+$  ions may also facilitate the activation of CO to form pentacoordinated carbonyl complex  $C_6$  by easily abstracting  $Cl^-$  ligand from the coordination sphere of  $C_5$ . Upon migratory insertion, the carbonyl complex forms the acyl complex  $C_7$ . During migratory insertion, a vacant site will be created at the fifth coordination site and will normally be occupied by a water molecule. The acyl complex  $C_7$  on reductive elimination of the acyl ligand and water molecule forms the product, thereby regenerating the active catalyst species  $C_4$ .

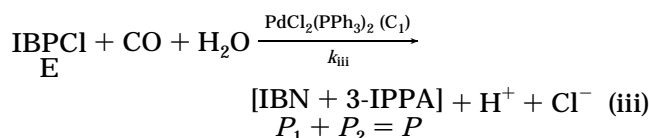
### Kinetic Modeling

**Empirical Model.** The following simplified reaction steps (steps i–iii) were considered to interpret the kinetics of the various reactions.

### Scheme 3. Reaction Mechanism



Carbonylation step



For the carbonylation step [reaction (iii)], an empirical rate equation based on observed trends of the average

rate of carbonylation as given below was considered.

$$r_A = \frac{k_{iii}[E_1][H_2O]A^*C_1^m}{1 + K[E_1]} \quad (2)$$

For other steps [i.e., reactions (i) and (ii)], the following rate equations were considered.

$$r_i = k_i[B_1][H^+] \quad (3)$$

$$r_{ii} = k_{ii}[D_1][H^+][Cl^-] \quad (4)$$

$$r_{-ii} = k_{-ii}[E_1] \quad (5)$$

The mass balance for reactants and products in a semibatch reactor with the kinetic resistance controlling and isothermal conditions can be represented by the following set of material balance equations.

$$-\frac{dB_1}{dt} = r_i = k_i[B_1][H^+] \quad (6)$$

$$\frac{dD_1}{dt} = r_i - r_{ii} + r_{-ii} = k_i[B_1][H^+] - k_{ii}[D_1][H^+][Cl^-] + k_{-ii}[E_1] \quad (7)$$

$$\frac{dE_1}{dt} = r_{ii} - r_{-ii} - r_A = k_{ii}[D_1][H^+][Cl^-] - k_{-ii}[E_1] - \frac{k_{iii}[E_1][H_2O]A^*C^m}{1 + K[E_1]} \quad (8)$$

$$\frac{dP_1}{dt} = r_A = \frac{k_{iii}[E_1][H_2O]A^*C^m}{1 + K[E_1]} \quad (9)$$

The initial conditions are

$$\text{at } t = 0, B = B_0, D_1 = 0, E_1 = 0, \text{ and } P_1 = 0 \quad (10)$$

In eqs 6–9,  $r_i$ ,  $r_{ii}$ , and  $r_A$  represent the reaction rates of

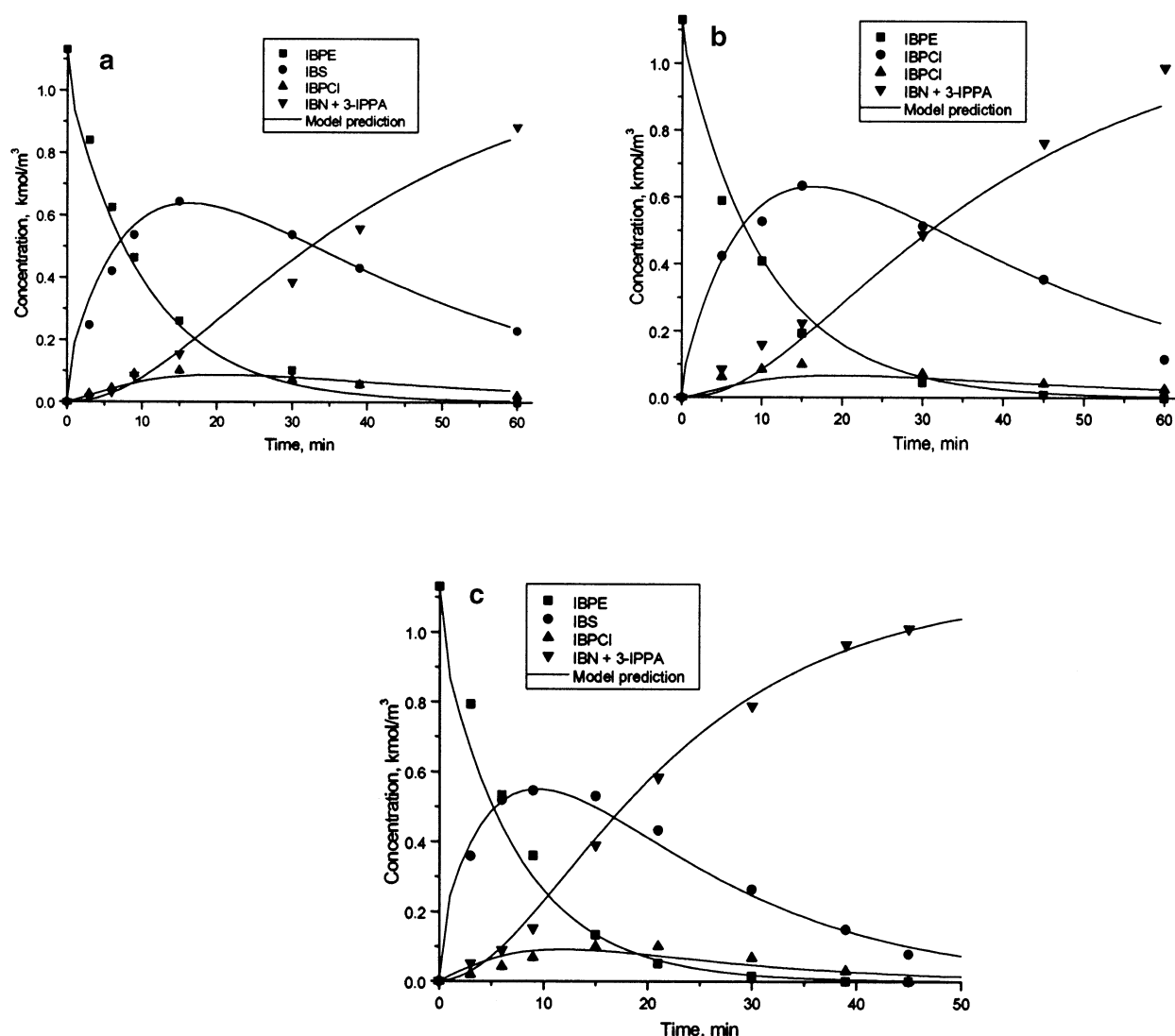


**Figure 7.** Comparison of experimental and model predictions: (a) 378 K; (b) 388 K; (c) 398 K. Reaction conditions: IBPE, 1.123 kmol/m<sup>3</sup>; TsOH/LiCl (1:1), 0.121 kmol/m<sup>3</sup>;  $P_{CO}$ , 5.4 MPa;  $PdCl_2(PPh_3)_2$ ,  $1.121 \times 10^{-3}$  kmol/m<sup>3</sup>;  $PPh_3$ ,  $2.242 \times 10^{-3}$  kmol/m<sup>3</sup>; water, 2.67 kmol/m<sup>3</sup>; MEK,  $1.95 \times 10^{-5}$  m<sup>3</sup>.

**Table 3. Kinetic Parameters**

temp (K)	$k_1 \times 10^2$ [m <sup>3</sup> /(kmol·s)]	$k_2 \times 10^2$ [(m <sup>3</sup> /kmol) <sup>2</sup> /s]	$k_3 \times 10^2$ [m <sup>3</sup> /(kmol·s)]	$k_4 \times 10^2$ [(m <sup>3</sup> /kmol) <sup>2.43</sup> /s]	$K$ (m <sup>3</sup> /kmol)
378	0.35	1.24	0.19	2.35	0.51
388	0.70	1.30	0.38	6.29	0.51
398	0.98	2.76	0.68	9.72	0.51

steps i–iii, respectively,  $r_{-ii}$  is the rate of the reverse reaction in step ii, and  $k_i$ ,  $k_{ii}$ ,  $k_{-ii}$ , and  $k_{iii}$  represent the respective rate constants for reactions shown in Scheme 4.  $K$  is an empirical constant,  $m$  is the reaction order with respect to catalyst,  $A^*$  is the saturation solubility of CO,  $B_i$ ,  $D_i$ ,  $E_i$ , and  $P_i$  are the concentrations of IBPE, IBS, IBPCL, and total amount of carbonylated products (IBN + 3-IPPA), respectively, and  $C_1$  is the concentration of catalyst charged.

Equations 6–9 describe the variation of the concentrations of IBPE, IBS, IBPCL, and the total carbonylated product (IBN + 3-IPPA) as a function of time. For a given set of initial conditions as described by eq 10, the above set of ordinary differential equations (eqs 6–9) can be solved to predict the concentration versus time behavior for the carbonylation of IBPE. This requires approximate initial guess estimates for the kinetic parameters which were calculated from the approximate

values of the local rates of formation of IBS, IBPCL, and the total carbonylation products (IBN and 3-IPPA) using the data at specific times of the concentration versus time profiles. To optimize the rate parameters, a computer program based on Marquart's method (optimization) combined with a fourth-order Runge–Kutta method (for solving the differential equations) was implemented. The concentration versus time profiles were simulated at various conditions and compared with experimental data. In the optimization procedure, a parameter,  $\phi_{min}$ , defined as follows was minimized.

$$\phi_{min} = \sum_{i=1}^{ns} \sum_{j=1}^{nt} (Y_{ij,exp} - Y_{ij,mod})^2 \quad (11)$$

where  $ns = 4$  and  $nt =$  number of experimental points. In eq 11,  $Y_{ij,exp}$  is the measured concentration of compon-

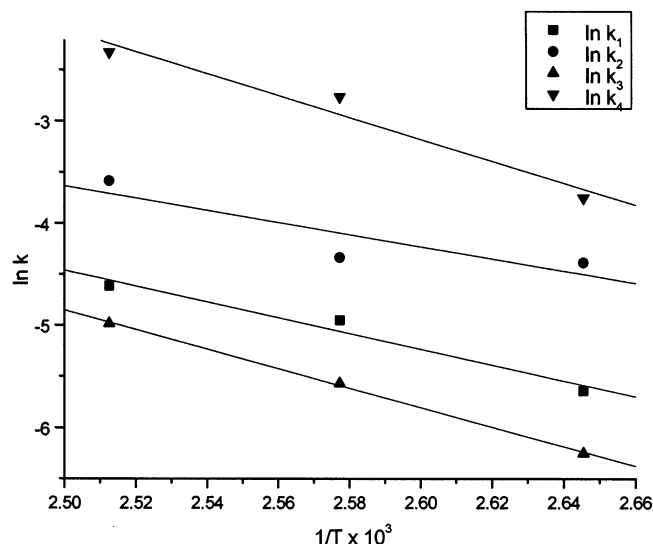


Figure 8. Temperature dependence of the rate parameters.

ent  $i$ ,  $Y_{ij,mod}$  is the calculated concentration of component  $i$ , and  $nt$  is the number of data points considered.

Following the above procedure, optimum values of the rate parameters were determined and are presented in Table 3. The  $\phi_{min}$  values were in the range of  $7 \times 10^{-4}$ – $8 \times 10^{-5}$ . A comparison between experimental data and model predictions is shown in Figure 7 for a few cases, though the predictions agreed over the entire range (Table 1) investigated. The experimental and predicted concentration–time data were found to agree within 5–10% error with the exception of a few points.

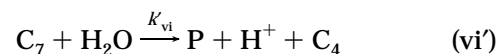
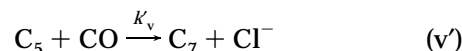
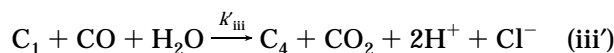
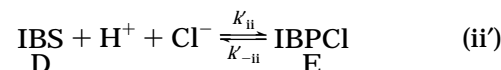
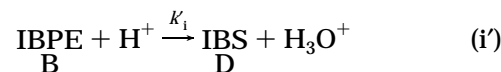
From the temperature dependence of rate constants,  $k_i$ ,  $k_{ii}$ ,  $k_{-ii}$ , and  $k_{iii}$  and using the Arrhenius law (see Figure 8), the respective activation energies were determined as 64.35, 49.49, 79.29, and 89.08 kJ/mol, while the values of preexponential factors are  $0.114 \text{ m}^3/(\text{kmol} \cdot \text{s})$ ,  $2.665 \times 10^{-2} (\text{m}^3/\text{kmol})^2/\text{s}$ ,  $7.878 \times 10^{-3} \text{ m}^3/(\text{kmol} \cdot \text{s})$ , and  $0.123 (\text{m}^3/\text{kmol})^{2.43}/\text{s}$ , respectively.

**Dynamic Model.** Even though the empirical rate model provided a reasonable representation of the concentration versus time data and the model proposed above could be useful for simulation of reactor performance, a more rigorous method would consider a molecular-level approach based on detailed stoichiometric reactions involved in the catalytic cycle as described in Scheme 2. Because the average rate of carbonylation shows first-order dependence on the concentration of water and a strong (0.8th order) dependence on the CO partial pressure as well as IBPE (0.7th order) concentration and 0.43th order with respect to the catalyst concentration, deriving a rate model assuming any one of the steps as the rate-determining step would not explain all of the observed trends. In this case, a dynamic analysis incorporating the variation of concentrations of all of the catalytic species, as well as the reaction intermediates with time, would be most suitable because it would allow consideration of more than one step as rate limiting. An attempt has been made to interpret the concentration versus time data for carbonylation of IBPE using a dynamic model for one specific case as described below.

To derive the rate equations, the following simplified reaction scheme was considered (Scheme 4). This reaction scheme involves all of the three principal steps of the reaction including (1) formation of IBPCL

(steps i' and ii'), (2) formation of the active catalytic species (step iii'), and (3) the main catalytic cycle (steps iv'–vi').

#### Scheme 4. Simplified Scheme for the Dynamic Model



The material balance equations that describe the concentration variation of IBPE, IBS, IBPCL, the carbonylation products, and the catalytic intermediates (Scheme 4) in a semibatch reactor are

$$-\frac{dB_1}{dt} = r'_i = k_i[B_1][\text{H}^+] \quad (12)$$

$$\frac{dD_1}{dt} = r'_i - r'_{ii} + r'_{-ii} = k_i[B_1][\text{H}^+] - k_{ii}[D_1][\text{H}^+][\text{Cl}^-] + k_{-ii}[E_1] \quad (13)$$

$$\frac{dE_1}{dt} = r'_{ii} - r'_{-ii} - r'_{iv} = k_{ii}[D_1][\text{H}^+][\text{Cl}^-] - k_{-ii}[E_1] - k_{iv}[E_1][C_4] \quad (14)$$

$$-\frac{dC_1}{dt} = r'_{iii} = k_{iii}[C_1][\text{CO}][\text{H}_2\text{O}] \quad (15)$$

$$\frac{dC_4}{dt} = r'_{iii} - r'_{iv} + r'_{vi} = k_{iii}[C_1][\text{CO}][\text{H}_2\text{O}] - k_{iv}[E_1][C_4] + k_{vi}[C_7][\text{H}_2\text{O}] \quad (16)$$

$$\frac{dC_5}{dt} = r'_{iv} - r'_v = k_{iv}[E_1][C_4] - k_v[C_5][\text{CO}] \quad (17)$$

$$\frac{dC_7}{dt} = r'_v - r'_{vi} = k_v[C_5][\text{CO}] - k_{vi}[C_7][\text{H}_2\text{O}] \quad (18)$$

$$\frac{dP_1}{dt} = r'_{vi} = k_{vi}[C_7][\text{H}_2\text{O}] \quad (19)$$

The initial conditions are

$$\text{at } t = 0, B_1 = B_0, D_1 = E_1 = P_1 = 0, C_1 = C_0, \text{ and } C_4 = C_5 = C_7 = 0 \quad (20)$$

In eqs 12–20,  $k_i$ ,  $k_{ii}$ ,  $k_{-ii}$ ,  $k_{iii}$ ,  $k_{iv}$ ,  $k_v$ , and  $k_{vi}$  represent the rate constants for steps i–vi as shown in Scheme 4,  $A^*$  is the saturation solubility of CO,  $B_0$  the initial concentration of IBPE,  $B_1$ ,  $D_1$ ,  $E_1$ , and  $P_1$  are the



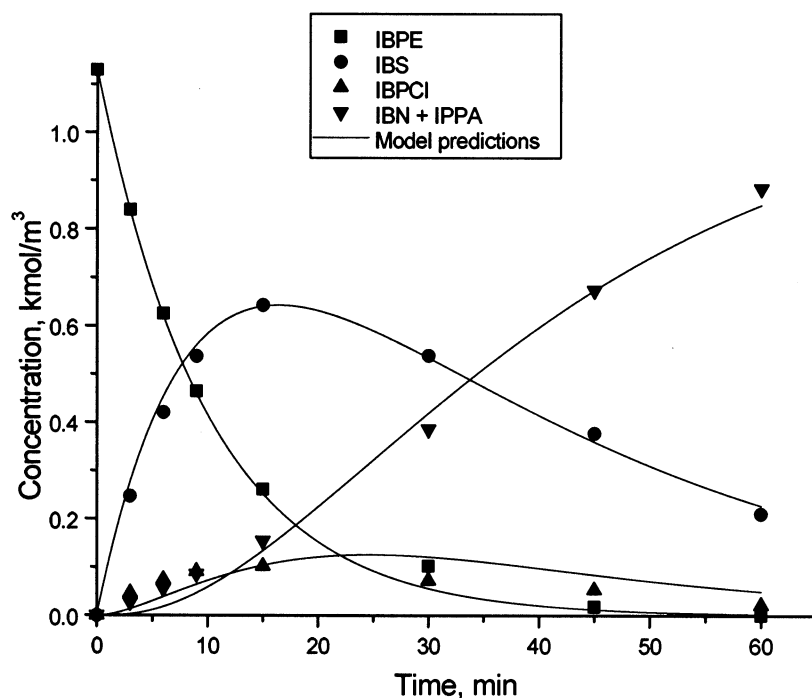


**Figure 9.** Comparison of experimental and predicted concentration–time profiles using the dynamic model. Reaction conditions: IBPE, 1.123 kmol/m<sup>3</sup>; TsOH/LiCl (1:1), 0.121 kmol/m<sup>3</sup>;  $P_{CO}$ , 5.4 MPa;  $PdCl_2(PPh_3)_2$ ,  $2.242 \times 10^{-3}$  kmol/m<sup>3</sup>;  $PPh_3$ ,  $2.242 \times 10^{-3}$  kmol/m<sup>3</sup>; water, 2.67 kmol/m<sup>3</sup>; MEK,  $1.95 \times 10^{-5}$  m<sup>3</sup>;  $T$ , 388 K.

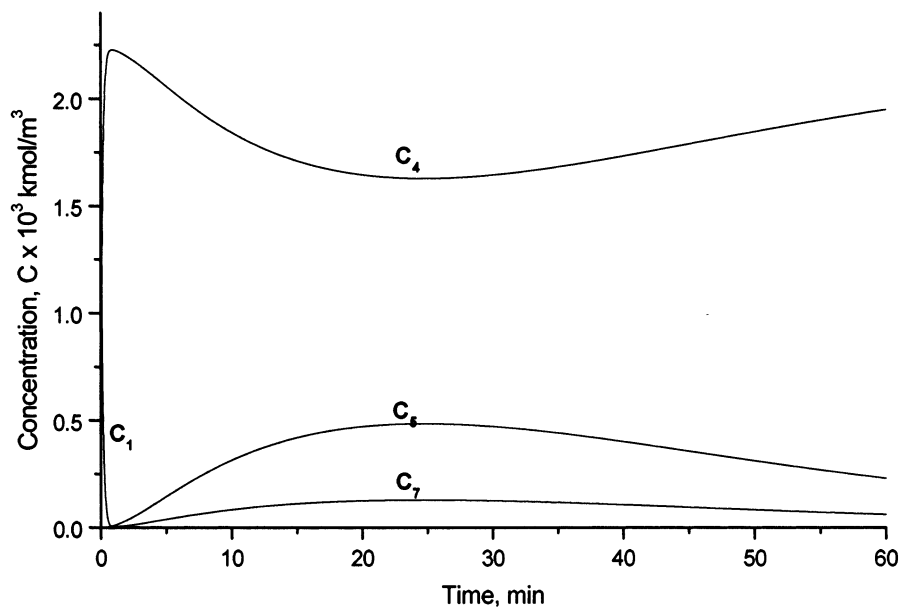


**Figure 10.** Predicted dynamic change in catalytic species concentration with time. Reaction conditions: IBPE, 1.123 kmol/m<sup>3</sup>; TsOH/LiCl (1:1), 0.121 kmol/m<sup>3</sup>;  $P_{CO}$ , 5.4 MPa;  $PdCl_2(PPh_3)_2$ ,  $2.242 \times 10^{-3}$  kmol/m<sup>3</sup>;  $PPh_3$ ,  $2.242 \times 10^{-3}$  kmol/m<sup>3</sup>; water, 2.67 kmol/m<sup>3</sup>;  $T$ , 388 K; MEK,  $1.95 \times 10^{-5}$  m<sup>3</sup>.

**Table 4.** Values of Rate Constants for the Dynamic Model (Equations 12–20)

parameter	value
$K'_i$ , (m <sup>3</sup> /kmol) <sup>2</sup> /s	$7.450 \times 10^{-3}$
$K'_{ii}$ , (m <sup>3</sup> /kmol) <sup>2</sup> /s	$1.250 \times 10^{-2}$
$K'_{-ii}$ , s <sup>-1</sup>	$1.600 \times 10^{-3}$
$K'_{iii}$ , m <sup>3</sup> /(kmol·s)	1.590
$K'_{iv}$ , (m <sup>3</sup> /kmol) <sup>2</sup> /s	0.150
$K'_{v}$ , (m <sup>3</sup> /kmol) <sup>2</sup> /s	0.214
$K'_{vi}$ , m <sup>3</sup> /(kmol·s)	0.952

concentrations of IBPE, IBS, IBPCL, and total amount of carbonylated products (IBN + 3-IPPA), respectively,  $C_0$  is the initial concentration of the catalyst, and  $C_1$ ,  $C_4$ ,  $C_5$  and  $C_7$  are the various catalytic species as shown in Schemes 2 and 4.

Equations 12–19 were solved using a fourth-order Runge–Kutta method using the initial conditions (eq 20) and initial estimates for the rate parameters. The  $\phi_{min}$  value is  $4.15 \times 10^{-4}$ , and the final optimized values of rate constants for the reaction conditions given in Figure 9 are shown in Table 4. A comparison of the experimental and predicted concentration–time data for a standard experiment using the dynamic model is shown in Figure 9.

In addition to the prediction of the concentrations of the reaction intermediates, the dynamic model can also be used for the prediction of the change of concentrations of different catalytic intermediates with time as shown in Figure 10.

The predicted concentration–time profile of the catalytic species using the dynamic model (Figure 10) shows that the catalytic species  $C_4$ ,  $C_5$ , and  $C_7$  are present in significant amounts at the present set of conditions, which also gives an indication of multiple steps as rate limiting. Considering the complexity involved in the dynamic model, a more rigorous analysis is required which needs an experimental technique to monitor active catalytic species,  $C_1$ ,  $C_4$ ,  $C_5$ ,  $C_7$ , etc., and a robust numerical/optimization technique. However, this approach will be more useful in understanding the dynamic changes in the concentration of catalytic species and the kinetics and mechanism on a molecular level.

## Conclusions

The carbonylation kinetics for IBPE were studied in a stirred semibatch reactor using a homogeneous  $\text{PdCl}_2(\text{PPh}_3)_2/\text{TsOH}/\text{LiCl}$  catalyst system over a temperature range of 378–398 K. The reaction orders for the carbonylation reaction were found to be 0.43, 1, 0.8, 0.7, and 1.2 for catalyst precursor, water, CO pressure, concentration of IBPE, and ratio of promoters ( $\text{TsOH}/\text{LiCl}$ ), respectively. It was shown that the rate data were in the kinetic regime and the gas–liquid mass-transfer resistance was negligible. The unusual fractional order with respect to catalyst, despite kinetic resistance control, indicates that the entire precursor is not present in the active form. A reaction pathway that consists of three different steps has been proposed that accounts for the formation of active palladium(0) species, active carbonylation substrate IBPCl and the principal catalytic cycle for carbonylation. A semibatch reactor model based on a simplified scheme considering the formation of IBS and IBPCl and the catalytic carbonylation of IBPCl as individual steps was used for the evaluation of kinetic parameters. The proposed rate model was found to describe satisfactorily the experimental concentration versus time profiles at all temperatures. The rate parameters were determined, and the activation energies corresponding to each rate constant were calculated. An attempt has also been made to develop a dynamic model considering the changes in the concentrations of all of the catalytic intermediate species along with reactants and products which indicated that, for complex reactions, more than one step may be rate limiting. The dynamic analysis would be more useful to understand the reaction mechanism on a molecular level.

## Nomenclature

- $A^*$  = saturation solubility of CO ( $\text{kmol}/\text{m}^3$ )  
 $B_1$  = concentration of 1-(4-isobutylphenyl)ethanol ( $\text{kmol}/\text{m}^3$ ), IBPE  
 $D_1$  = concentration of 4-isobutylstyrene ( $\text{kmol}/\text{m}^3$ ), IBS  
 $E_1$  = concentration of 1-(4-isobutylphenyl)ethyl chloride ( $\text{kmol}/\text{m}^3$ ), IBPCl  
 $B_0$  = initial concentration of 1-(4-isobutylphenyl)ethanol ( $\text{kmol}/\text{m}^3$ )  
 $P_1$  = total concentration of carboxylic acid formed (IBN + 3-IPPA) ( $\text{kmol}/\text{m}^3$ )  
 $C_1$  = concentration of the catalyst ( $\text{kmol}/\text{m}^3$ )

$r_i$ ,  $r_{ii}$ ,  $r_{-ii}$ ,  $r_A$  = reaction rates for steps i–iii in Scheme 3  
 $k_i$ ,  $k_{ii}$ ,  $k_{-ii}$ ,  $k_{iii}$  = reaction rate constants for steps i–iii in Scheme 3 (units as given in Table 3)

$r'_i$ ,  $r'_{ii}$ ,  $r'_{-ii}$ ,  $r'_{iii}$ ,  $r'_{iv}$ ,  $r'_v$ ,  $r'_{vi}$  = reaction rates for steps i'–vi' in Scheme 4

$K_i$ ,  $K_{ii}$ ,  $K_{-ii}$ ,  $K_{iii}$  = reaction rates for steps i'–vi' in Scheme 4 (units as given in Table 4)

$K$  = a constant in eq 1

$m$  = reaction order with respect to catalyst

$\phi_{\min}$  = parameter defined in eq 11

## Acknowledgment

A.M.S. and J.S. thank Council of Scientific and Industrial Research (CSIR), India, for a research fellowship.

## Literature Cited

- (a) Rieu, J. P.; Boucherle, A.; Cousse, H.; Mouzin, G. Methods For The Synthesis Of Antiinflammatory 2-Arylpropionic Acids. *Tetrahedron* **1986**, *42*, 4095. (b) Sheldon, R. A. Organic Synthesis—Past, Present and Future. *Chem. Ind.* **1992**, 903.
- Armor, J. N. New Catalytic Technology Commercialized in the USA during the 1980s. *Appl. Catal.* **1991**, *78*, 141.
- (a) Elango, V.; Murphy, M. A.; Mott, G. N.; Zey, E. G.; Smith, B. L.; Moss, G. L. (Hoechst Celanese Corp.). Method for Producing Ibuprofen. European Patent 400,892, 1990. (b) Seayad, A.; Kelkar, A. A.; Chaudhari, R. V. Carbonylation of *p*-Isobutylphenylethanol to Ibuprofen Using Palladium Catalyst: Activity and Selectivity Studies. *Stud. Surf. Sci. Catal.* **1998**, *113*, 883.
- (a) Alper, H.; Hamel, N. Asymmetric Synthesis of Acids by the Palladium-Catalyzed Hydrocarboxylation of Olefins in the Presence of (*R*)-(-) or (*S*)-(+)-1,1'-Binaphthyl-2,2'-diyl Hydrogen Phosphate. *J. Am. Chem. Soc.* **1990**, *112*, 2803. (b) Jang, E. J.; Lee, K. H.; Lee, J. S.; Kim, Y. G. Regioselective Synthesis of Ibuprofen via the Palladium Complex Catalyzed Hydrocarboxylation of 1-(4-Isobutylphenyl) Ethanol. *J. Mol. Catal. A: Chem.* **1999**, *138*, 25.
- Papadogianakis, G.; Maat, L.; Sheldon, R. A. Catalytic conversions in water. 5. Carbonylation of 1-(4-isobutylphenyl)ethanol to ibuprofen catalysed by water-soluble palladium–phosphine complexes in a two-phase system. *J. Chem. Technol. Biotechnol.* **1997**, *70* (1), 83.
- Seayad, A.; Jayasree, S.; Chaudhari, R. V. Highly Efficient Catalyst System For The Synthesis Of 2-Arylpropionic Acids By Carbonylation. *Catal. Lett.* **1999**, *61*, 99.
- Nair, V. S.; Matahew, S. P.; Chaudhari, R. V. Kinetics of Hydroformylation of Styrene Using Homogeneous Rhodium Complex Catalyst. *J. Mol. Catal. A: Chem.* **1999**, *143*, 99.
- Purvanto, P.; Deshpande, R. M.; Chaudhari, R. V.; Delmas, H. Solubility of Hydrogen, Carbon Monoxide, and 1-Octene In Various Solvents And Solvent Mixtures. *J. Chem. Eng. Data* **1996**, *41*, 1414.
- Ramachandran, P. A.; Chaudhari, R. V. *Three Phase Catalytic Reactors*; Gordon and Breach: New York, 1983.
- Seayad, A.; Jayasree, S.; Chaudhari, R. V. Carbonylation of 1-arylethanol using homogeneous Pd complex catalysts. *J. Mol. Catal. A: Chem.* **2001**, *172* (1–2), 151.
- Collman, J. P.; Hegedus, L. S. In *Principles and Applications of Organotransition Metal Chemistry*; Kelly, A., Ed.; University Science Books: CA, 1980.
- (a) Lau, K. S. Y.; Wong, P. K.; Stille, J. K. Oxidative Addition of Benzyl Halides to Zerovalent Palladium Complexes. Inversion of Configuration at Carbon. *J. Am. Chem. Soc.* **1976**, *98*, 5832. (b) Stille, J. K.; Lau, K. S. Y. Mechanisms of Oxidative Addition of Organic Halides to Group 8 Transition-Metal Complexes. *Acc. Chem. Res.* **1977**, *10*, 434.

(13) (a) Negishi, E. I.; Takahashi, T.; Akiyoshi, K. Bis-(Triphenylphosphine)Palladium—Its Generation, Characterization, and Reactions. *J. Chem. Soc., Chem. Commun.* **1986**, 1338. (b) Amatore, C.; Azzabi, M.; Jutand, A. Role and Effects of Halide Ions on the Rates and Mechanisms of Oxidative Addition of Iodobenzene to Low-Ligated Zerovalent Palladium Complexes Pd<sup>0</sup>-(Pph<sub>3</sub>)<sub>2</sub>. *J. Am. Chem. Soc.* **1991**, 113, 8375.

(14) Amatore, C.; Jutand, A. Intimate Mechanism of Oxidative Addition to Zerovalent Palladium Complexes in the Presence of

Halide Ions and Its Relevance to the Mechanism of Palladium-Catalyzed Nucleophilic Substitutions. *J. Am. Chem. Soc.* **1993**, 115, 9531.

*Received for review August 8, 2002*

*Revised manuscript received November 20, 2002*

*Accepted November 25, 2002*

IE020628D